Study of jet production in p-N interactions at $\sqrt{s} \approx 500$ GeV in EAS multicore events

The EAS-TOP Collaboration

M.Aglietta[1,2], B.Alessandro[2], P.Antonioli[3], F.Arneodo[4], L.Bergamasco[2,5], M.Bertaina[2,5], C.Castagnoli[1,2], A.Castellina[1,2], A.Chiavassa[2,5], G.Cini Castagnoli[2,5], B.D'Ettorre Piazzoli[6], G.Di Sciascio[6], W.Fulgione[1,2], P.Galeotti[2,5], P.L.Ghia[1,2], M.Iacovacci[6], G.Mannocchi[1,2], C.Morello[1,2], G.Navarra[2,5], L.Riccati[2], O.Saavedra[2,5], G.C.Trinchero[1,2], S.Valchierotti[2,5], P.Vallania[1,2], S.Vernetto[1,2] and C.Vigorito[1,2]

[1]*Istituto di Cosmo−Geofisica del CNR, Torino, Italy*

[2]*Istituto Nazionale di Fisica Nucleare, Torino, Italy*

[3]*Istituto Nazionale di Fisica Nucleare, Bologna, Italy*

[4]*INFN, Laboratorio Nazionale del Gran Sasso, L' Aquila, Italy*

[5]*Dipartimento di Fisica Generale dell' Università, Torino, Italy*

[6]*Dipartimento di Scienze Fisiche dell' Università and INFN, Napoli, Italy*

Abstract

The cross section for large p_t jet production for transverse momentum $10 \leq p_t \leq 20\ GeV/c$ and rapidity interval $1.6 \leq \eta \leq 2.6$ in p-N ("Air") interactions is studied from the analysis of multicore Extensive Air Showers recorded in the EAS-TOP calorimeter. The projectiles are the leading particles interacting at atmospheric depths between 250 and $390\ gcm^{-2}$, the CMS energy of interaction being $\sqrt{s} \approx 500\ GeV$. The measured jet production cross section in $p-N$ interactions, with respect to $p-p$ interactions, is: $(d\sigma/dp_t)^{jet}_{pN} = (d\sigma/dp_t)^{jet}_{pp} \cdot A^{\alpha}$ with $\alpha = 1.56 \pm 0.07$ for $A = 14.7$ (average mass number of "air" nuclei). Such value is compatible within the experimental uncertainties with the one obtained in $p-nucleus$ accelerator measurements at $\sqrt{s} \simeq 30\ GeV$ in the same range of transverse momentum and rapidity interval.

1 Introduction:

Jet production is studied at colliders in $p-\bar{p}$ interactions up to $\sqrt{s} \simeq 630\ GeV$ [1,2] and $\sqrt{s} \simeq 1.8\ TeV$ [3] and in $p-nucleus$ interactions in fixed target experiments up to $\sqrt{s} \simeq 30\ GeV$ [4,5].

In Extensive Air Shower (EAS) experiments multicore events (i.e. events with multiple structure in the e.m. component near the axis) have been observed since '60's [6-10] and their interpretation as due to jet production has lead to first information on production cross sections [10]. The consistency of the observations in different cosmic rays experiments has been recently discussed in [11,12]. In the case of multicore EAS, the jet is essentially produced by the leading particle interactions at intermediate altitudes in the atmosphere ($z \approx 6 - 12\ km$ above sea level) at typical energies $\sqrt{s} \approx (300 - 1000)\ GeV$. Such experiments allow thus the extension of $p-nucleus$ accelerator data and the direct comparison with $p-\bar{p}$ collider measurements.

From the point of view of cosmic rays physics, the effect can be relevant for experiments exploiting the high energy component in the core region to derive conclusions on the cosmic ray primary composition.

2 The experiment:

The measurement is performed by means of the EAS-TOP array located at Campo Imperatore, central Italy, $2005\ m\ a.s.l.$ (National Gran Sasso Laboratories). EAS core investigations are performed by means of its calorimeter [13]. Shower sizes and arrival directions are obtained from the electromagnetic detector [14].

The EAS-TOP calorimeter is a parallelepiped of dimensions $(12 \times 12 \times 3)\ m^3$ and consists of 9 identical planes. Each active plane is made of two *streamer* tube layers for muon tracking and one layer of *quasi proportional* tubes ($3 \times 3\ cm^2$ section, $12\ m$ length) for hadron calorimetry, separated by $13\ cm$ thick iron absorbers, for a total depth of 818 $g\ cm^{-2}$, i.e.$\simeq 6.2$ nuclear mean free paths. The read-out of the quasi proportional tubes

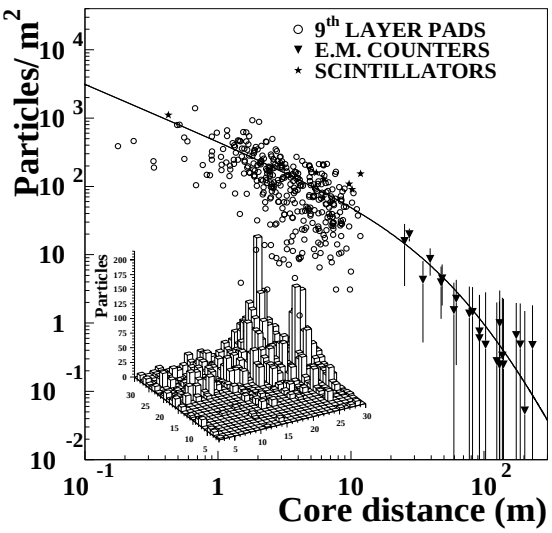

Figure 1: A multicore EAS: the reconstructed l.d.f of the main shower and the central region are shown.

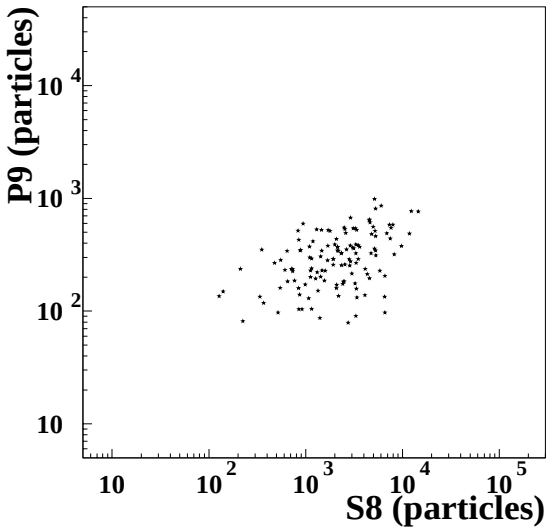

Figure 2: Scatter plot of cluster patterns (P_9,S_8) of the detected secondary structures in 130 multicore EAS.

is performed by induction through a matrix of 840 pads ($40 \times 38\ cm^2$) placed on top of each level for a total area of $128\ m^2$. The active layers of the upper plane (9^{th}) are unshielded and operate as a fine grain detector of the electromagnetic component of EAS cores. A model of the response of the *quasi proportional* chambers has been developed and checked through on site measurements and a test at CERN facilities with a $50\ GeV\ e^+$ beam. Eight ($80 \times 80\ cm^2$) scintillator counters, identical to the ones of the EAS-TOP e.m. detector are located above the 9^{th} plane: 4 internal (P_i) are placed at about $3\ m$ from the calorimeter center and 4 external (M_i) outside the module structure at its corners. They are used to select contained EAS cores.

3 The data:

In the present analysis only Extensive Air Showers which triggered both the electromagnetic and hadronic detectors have been considered: 5322 events in the size range $10^{5.26} \leq N_e \leq 10^{5.60}$, i.e. primary energy [1] between 500 and $1000\ TeV$ for primary protons. EAS with core hitting the calorimeter are first selected with scintillators (M_i, P_i) using the condition: $R = \frac{\sum_{i=1}^{4} M_i}{\sum_{i=1}^{4} P_i} \leq 1$. The shower size and core location are reconstructed through a fit to the NKG theoretical particle distribution[2] of the recorded particle densities in the upper level (with pad recorded particle numbers $N_{i,j}$), the M_i and P_i scintillators and the e.m. counters of the array. Events with core located inside a fiducial area of $8 \times 8\ m^2$ centered on the calorimeter and with zenith angle $\theta \leq 35^0$ are selected for further analysis. For shower size $N_e \geq 10^5$ the reconstruction efficiency is $\epsilon \geq 95\%$, the resolution $\frac{\Delta N_e}{N_e} \leq 15\%$ and the accuracy on arrival direction $\sigma_\theta \approx 0.5^0$; in 70% of events the fitted core position is found at a distance $d \leq 70\ cm$ from the pad with maximum recorded particle density. First each event is fully reconstructed, as previously described, to get shower size, core location, arrival direction and lateral distribution function. The core location (see figure 1), shower size (N_e) and slope (s) of l.d.f. provide the expected average number of particles $\overline{N}_{i,j}$ and therefore the corresponding fluctuation ($\sigma_{i,j}(\overline{N}_{i,j})$) on each (i,j) pad of the unshielded layer. Then by applying a cluster algorithm to the matrix of the quantities $S_{i,j} = \frac{N'_{i,j}}{\sigma_{i,j}(\overline{N}_{i,j})}$ with $(N'_{i,j} = N_{i,j} - \overline{N}_{i,j})$ (1) subcore structures in the e.m. component are extracted by selecting the maximum

[1] The size to energy conversion expression used is: $E_0(TeV) = \alpha \cdot {N_e}^{\beta}$ with $\alpha = 0.0093$ and $\beta = 0.903$, obtained by means of a simulation (CORSIKA-HDPM [15]) for primary protons [16].

[2] $\rho(r) = \frac{Ne}{(r_0)^2}(1 + \frac{r}{r_0})^{s-4.5}(\frac{r}{r_0})^{s-2}$, with shower size N_e, slope s and $r_0 \approx 100\ m$ [17].

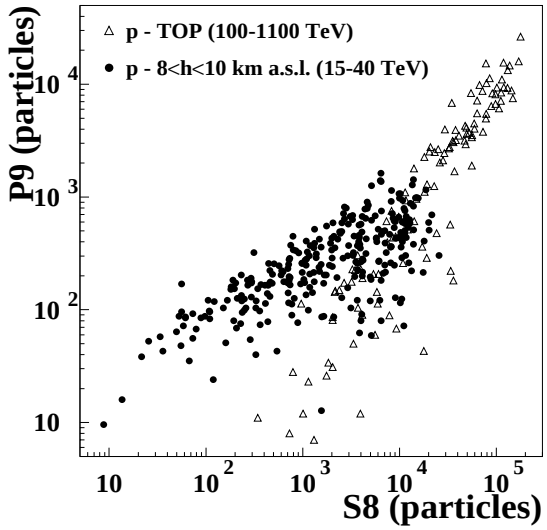

Figure 3: Scatter plot of cluster patterns (P_9,S_8), showing the difference between showers initiated at the top and at lower atmospheric levels.

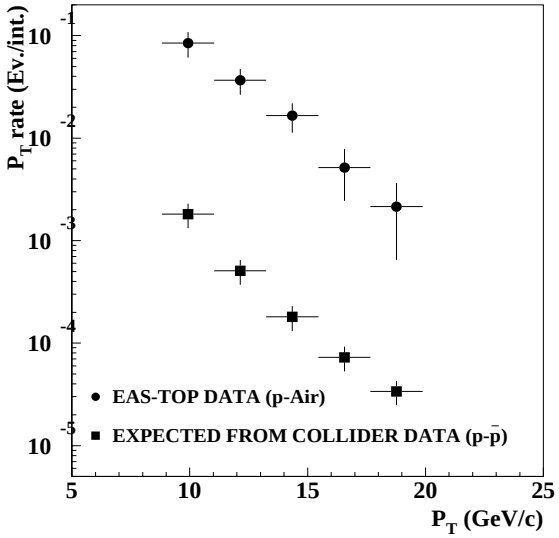

Figure 4: Measured p_t rate in multicore EAS compared with the expected one from $p-\bar{p}$ collider cross section data.

value of $\sum S_{i,j} = S_{max}$. The contribution of false clusters, due to pad response fluctuations in single core events and recognized by the algorithm, has been evaluated by means of a simulation: values of $S_{max} > 20$ identify physical events. For the energy and production height determination of each subcore, the quantities: $P_9 = \sum_{(i,j)}^{20} N'_{i,j}$ at the uppermost level (i.e. the electromagnetic content) and $S_8 = \sum_{k=1}^{8} \sum_{(i,j)}^{20} N'_{i,j,k}$ ($N'_{i,j}$ defined for each layer k as in expression (1)) integrated over the 8 internal layers (i.e. the hadronic and high energy e.m. contents), are used. The sum involves the 20 most significant pads inside the structure within $1\ m$ from the subcore position on the uppermost plane and, for internal ones, from its rojected position following the EAS direction. For internal layers $\overline{N}_{i,j}$ is obtained from the pads at the same distance r from the main core, not belonging to the subcore structure. The resulting scatter plot P_9-S_8 for physical events is shown in figure 2. The same plot is shown in figure 3 for simulated primary proton showers of different energies initiated at the top and at different atmospheric depths ranging from 6000 to $12000\ m\ a.s.l.$. From the comparison of figures 2 and 3 it results that the pattern of the selected subcore structures falls in the region characterized by intermediate starting levels in the atmosphere. Top events are excluded since they are expected to have a much higher hadronic content for the same electromagnetic size (while the main shower core in the P_9-S_8 parameters space of the selected EAS agrees with the expectations for showers initiated at the top). This proves that the subcores are produced by interactions in the cascade development in the atmosphere occurring at altitudes $\bar{h} \approx 7000\ m$ above the detector. Subcore energies and production heights are obtained through a fit to the quantities P9 and S8 (for details see [21]). Typical values are: $10 \leq E_s \leq 50\ TeV$ and $4 \leq h \leq 10\ Km$ above the detectors while distances from axis are $1.5 \leq r \leq 7\ m$. By means of ad hoc simulations the following quantities have been computed and included in the analysis: a) the energy collection efficiency $\epsilon_E \simeq 86\%$, due to the jet fragmentation, to be applied to the subcore energy E_s; b) the efficiency for subcore detection $\epsilon_D(N_e, E_s, r)$; c) the geometrical rapidity acceptance $\epsilon_R(\eta)$. The transverse momentum for each subcore has been obtained using the expression: $p_t^{meas} = \frac{E_s \cdot r}{\epsilon_E \cdot \bar{h}}$. The uncertainty in the p_t^{meas} measurements is: $\Delta p_t^{meas}/p_t^{meas} \approx 50\%$. At the quoted intermediate interaction levels the projectiles contributing to the events can be associated to the leading particles inside the showers. Their energy spectrum has been derived from the primary one by scaling the corresponding energy to the mean production depth of our events with an attenuation length $\Lambda \approx 100\ gcm^{-2}$. At the mean production height $z \approx 9000\ m\ a.s.l.$, i.e. atmospheric depth $X \approx 270\ gcm^{-2}$, the leading particle energy, averaged over the primary spectrum in the range $500 - 1000\ TeV$ here analysed, is $E_{l.p} \approx 125\ TeV$

corresponding to $\sqrt{s} \approx 500\ GeV$ for $p-p$ interactions. The accepted region of pseudo-rapidity in which $\epsilon_R(\eta)$ exceeds 40% is $7.8 \leq \eta \leq 8.8$: it corresponds to $1.6 \leq \eta_{c.m.} \leq 2.6$ in the c.m. of the interaction.

4 The results:

The rate of large p_t events per interaction is obtained by applying to each event the detection efficiency $\epsilon_d(N_e, E_s, r)$ and the geometrical acceptance $\epsilon_R(\eta)$. The reported uncertainty in the measurement of transverse momentum, together with the steepness of the slope of the p_t distribution ($f(p_t) \propto p_t^{-\gamma}$) introduces a systematic overestimate of the transverse momentum, so that $p_t^{meas} = (1.35 \pm 0.05) \cdot p_t$ (for $\gamma = 6.04 \pm 0.56$ obtained from the fit to the experimental data). The individual p_t^{meas} values have therefore been shifted of this factor. The obtained p_t distribution is shown in figure 4. In the same figure, the p_t rate distribution, calculated from the collider $p-\bar{p}$ cross section data $d\sigma/dp_t$ [3] at $\sqrt{s} \approx 500\ GeV$ in the same rapidity interval assuming as target nuclei single protons, is shown. Statistical and systematic errors are shown. The slopes of the two distributions, $f(p_t) \propto p_t^{-\gamma}$, with $\gamma = 6.16 \pm 0.09$ for the calculated one for $p-\bar{p}$ interactions, and $\gamma = 6.04 \pm 0.56$ for the experimental one for $p-N$ interactions, are in agreement inside the experimental errors, showing that the p_t dependencies of $p-\bar{p}$ and $p-N$ cross sections are compatible. The gap in the absolute rates reflects the difference between $p-p$ and $p-N$ cross sections. The ratio $R = (d\sigma/dp_t)^{jet}_{pN}/(d\sigma/dp_t)^{jet}_{pp}$ is constant versus the transverse momentum and is on average: $\bar{R} = 60.4 \pm 12.9$. By representing such gap following the usual expression $(d\sigma/dp_t)^{jet}_{pN} = (d\sigma/dp_t)^{jet}_{pp} \cdot A^{\alpha}$ with $A = 14.7$ the value $\alpha = 1.56 \pm 0.07$ is obtained. Such value agrees with accelerator data (ranging from $\alpha \simeq 1.37$ and $\alpha \simeq 1.55$ for Pb and Al target [5,18-20] at $< p_t^{jet} >= 12.1\ GeV/c$ mean value of our measurements) obtained at $\sqrt{s} \simeq 30\ GeV$ in the same range of transverse momentum and pseudo-rapidity, showing that no change in the target mass number dependence of jet production cross sections occurs between $\sqrt{s} \simeq 30\ GeV$ and $\sqrt{s} \simeq 500\ GeV$.

References

[1] Appel J.A. et al., Phys. Lett. B, 160, (1985), 349
[2] Di Lella L., Ann. Rev. Nucl. Part. Sci., 35, (1985), 107
[3] Abe F. et al., Phys. Rev. Lett., 65, (1990), 968
[4] Cronin J.W. et al., Phys. Rev. D, 11, (1975), 3105
[5] Gomez R. et al., Phys. Rev. D, 35, (1987), 2736 and references therein
[6] Hazen W.E. and Heineman R.E., Phys. Rev., 90, (1953), 496
[7] Matano T. et al., Canad. J. Phys., 46, (1968), S56
[8] Bakich A.M. et al., Canad. J. Phys., 46, (1968), S30
[9] Bosia G. et al., Il Nuovo Cimento C, 3, (1980), 215
[10] Chudakov A.E. et al., Proc. XVII ICRC, Paris, 6, (1981), 183
[11] Aglietta M. et al., Nuovo Cimento C, 18, (1995), 663
[12] Lidvansky A.S., Proc. XXV ICRC, Durban, 6, (1997), 169
[13] The EAS-TOP Collaboration, Nucl. Instr. and Meth. A, 420, (1999), 117
[14] Aglietta M. et al., Nucl. Instr. and Meth. A, 336, (1993), 310
[15] Capdevielle J.N. et al., KFK Report 4998, (1992)
[16] Aglietta M. et al., Proc. XXV ICRC, Durban, 4, (1997), 125
[17] Kamata K. et al., Suppl. Progr. Theor. Phys., 6, (1958), 93
[18] Brown B. et al., Phys. Rev. Lett., 50, (1983), 11
[19] Miettinen H. et al., Nucl. Phys. A, 418, (1984), 315
[20] Hsiung Y.B. et al., Phys. Rev. Lett., 55, (1985), 457

[3] The invariant cross section used is: $\frac{Ed^3\sigma}{dp^3} = p_t^{-n} f(x_t)$ with $f(x_t) = C\frac{(1-x_t)^m}{x_t^2}$, $n = 4.74 \pm 0.06$, $m = 6.54 \pm 0.15$, $C = (8.3 \pm 0.4) \cdot 10^{-29}\ cm^2 GeV^{n-2}$ and $x_t = 2p_t/\sqrt{s}$ [1].